PHYSICAL REVIEW D **88,** 116002 (2013)

J/ψ in high-multiplicity pp collisions: Lessons from pA collisions

B. Z. Kopeliovich,[1] H. J. Pirner,[2] I. K. Potashnikova,[1] K. Reygers,[3] and Iván Schmidt[1]

[1]*Departamento de Física, Universidad Técnica Federico Santa María and Centro Científico-Tecnológico de Valparaíso, Avenida España 1680, 239-0123 Valparaiso, Chile*

[2]*Institute for Theoretical Physics, University of Heidelberg, Philosophenweg 19, D-69120 Heidelberg, Germany*

[3]*Physikalisches Institut, University of Heidelberg, Im Neuenheimer Feld 226, D-69120 Heidelberg, Germany*

(Received 22 August 2013; published 2 December 2013)

Gluons at small x in high-energy nuclei overlap in the longitudinal direction, so the nucleus acts as a single source of gluons, like higher Fock components in a single nucleon, which contribute to inelastic collisions with a high multiplicity of produced hadrons. This similarity helps to make a link between nuclear effects in pA and high-multiplicity pp collisions. Such a relation is well confirmed by data for the J/Ψ production rate in high-multiplicity pp events measured recently in the ALICE experiment. Broadening of J/Ψ transverse momentum is predicted for high-multiplicity pp collisions.

DOI: 10.1103/PhysRevD.88.116002 PACS numbers: 11.80.La, 12.38.Qk, 12.40.Nn, 13.85.Hd

I. INTRODUCTION

Hadron multiplicities larger than the mean value in pp collisions can be reached due to the contribution of higher Fock states in the proton, containing an increased number of gluons. Correspondingly, the relative rate of J/Ψ production will also be enhanced, because heavy flavors are produced more abundantly in such gluon-rich collisions.

We define the ratios of measured multiplicity to average multiplicity in pp collisions per unit of rapidity as R, and differentiate between the general hadron multiplicity ratio R_h and the J/Ψ ratio $R_{J/\Psi}$:

$$R_h^{pp} \equiv \frac{dN_h^{pp}/dy}{\langle dN_h^{pp}/dy\rangle}, \tag{1}$$

$$R_{J/\Psi}^{pp} \equiv \frac{dN_{J/\Psi}^{pp}/dy}{\langle dN_{J/\Psi}^{pp}/dy\rangle}. \tag{2}$$

The denominators in (1) and (2) are the mean charge hadron multiplicity and the mean J/Ψ multiplicity per event averaged over events with different hadron multiplicities.

More gluons participating in collisions with $R_h^{pp} > 1$ explain why $R_{J/\Psi}^{pp}$ rises with increasing R_h. Of course such fluctuations are rare. The absolute value of the J/Ψ production rate in such rare events might be very low. Although qualitatively such a correlation is rather obvious, its quantitative description is far from being trivial. In this paper we outline and employ a close relation between the $R_{J/\Psi}^{pp} - R_h^{pp}$ correlation in pp and pA collisions.

In a boosted high-energy nucleus, the longitudinal distances between the bound nucleons are contracting with the Lorentz factor m/E, while the small-x glue in each nucleon contracts much less, as m/xE [1]. For instance, in a collision at the c.m. energy $\sqrt{s}$ of LHC at the midrapidity, $x = 2\sqrt{\langle k_T^2\rangle}/\sqrt{s} \sim 10^{-4}$, where $\langle k_T^2\rangle \approx 0.5\ \mathrm{GeV}^2$ is the mean transverse momentum squared of gluons. So gluons stick out far from the Lorentz contracted nuclear disc. In the nuclear rest frame the same effect is interpreted as a long lifetime of the gluon cloud, which propagates in the longitudinal direction over the distance $\sqrt{s}/\langle k_T^2\rangle$, four orders of magnitude longer than the mean internucleon spacing in nuclei at LHC energies. Therefore, all gluons that overlap in the transverse plane also overlap longitudinally. Thus, they can be treated as a single gluon cloud originating from one source with increased density, equivalent to higher Fock states in a single nucleon.

We claim that one can emulate the dependence of $R_{J/\Psi}^{pp}$ on R_h^{pp} in high-multiplicity pp collisions by the analogous correlation in pA collisions. In the latter case, one can use as the numerators in the ratios (1) and (2) the mean multiplicities of light hadrons and J/Ψ measured in pA collisions, while the denominators remain the same as in (1) and (2), so they are also here the mean hadron and the J/Ψ multiplicities in pp collisions.

II. HIGH-MULTIPLICITY EVENTS IN pp AND pA COLLISIONS

Multiplicity distributions in pp and pA collisions at high energies have been studied [2–4] within Regge phenomenology, based on the Abramovsky-Gribov-Kancheli (AGK) cutting rules [5]. The simultaneous unitarity cut of elastic pp amplitude through n Pomerons corresponds to the production of n showers of particles, i.e. to a multiplicity n times higher than in one cut Pomeron. Weight factors for these graphs are usually estimated either within the eikonal model (see Fig. 1, left), or in the quasi-eikonal approximation [6], taking into account intermediate diffractive excitations.

Particle production in pA collisions has many similarities to high-multiplicity pp events. The Glauber model, equipped with the AGK rules, corresponds also to the eikonal graphs in Fig. 1 (left). However, in pA collisions the Pomerons are attached to different nucleons in the

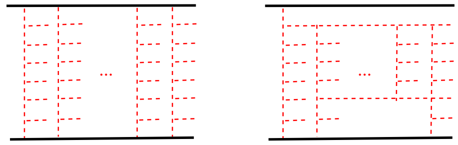

FIG. 1 (color online). Amplitude of multiple production corresponding to n cut Pomerons in the eikonal approximation (*left*), and including the Landau-Pomeranchuk coherence effects (*right*).

nuclear target. For this reason high-multiplicity events in pA collisions are enhanced, because the weight factors are different from pp, and the graph with n cut Pomerons (production of n showers) contains the factor $A^{n/3}/n!$. As a result, the inclusive cross section of particle production acquires no nuclear shadowing [7,8]. The mean number of produced showers, the so-called number of collisions,

$$N_{\rm coll} \equiv A\frac{\sigma_{\rm in}^{pN}}{\sigma_{\rm in}^{pA}}, \tag{3}$$

and the mean hadron multiplicity increases as $A^{1/3}$. The nuclear ratio $R_h^{pA} = \langle dN_h^{pA}/dy\rangle/\langle dN_h^{pp}/dy\rangle$ is defined as a ratio of the mean hadron multiplicities in pA to pp collisions. In the Glauber eikonal model, it is given by the number of collisions,

$$(R_h^{pA})_{\rm Gl} = N_{\rm coll}. \tag{4}$$

However, comparison with data shows that this relation significantly overestimates the hadron multiplicity. The popular parametrization for the nuclear effects,

$$R_h^{pA} = 1 + \beta(N_{\rm coll} - 1), \tag{5}$$

shows, when fitted to data, that $\beta < 1$ [9].

The eikonal Glauber approximation Eq. (4) ignores several corrections. Energy conservation shrinks the allowed energy interval with a rising number of cut Pomerons [10]. The source partons, i.e. the valence and sea quarks, which participate in the multi-Pomeron exchange, are distributed in rapidity, and this affects the energy and multiplicity in each cut Pomeron. This is taken into account in the quark-gluon string [11] or dual parton [12] models, which describe quite well multiple hadron production [13,14].

Another source of reduction of multiplicity are coherence effects. The eikonal description relies on the Bethe-Heitler regime of radiation illustrated in Fig. 1 (left). However, amplitudes of gluon radiation from inelastic interactions on different nucleons interfere, leading to a damping of the radiation spectrum, known as the Landau-Pomeranchuk suppression, or gluon shadowing. The related radiation pattern is illustrated in Fig. 1 (right). Maximal suppression occurs when the gluon density [15,16] saturates, which leads to a modification of the transverse momentum distribution of gluons called color glass condensate [17].

A comprehensive analysis of data [18] from fixed-target experiments led to $\beta = 0.59 \pm 0.01$. The recent analysis of data in [19], at $\sqrt{s} < 200$ GeV, found good agreement with the simple behavior $R_h^A = \frac{1}{2}N_{\rm part}$, where the number of participants for pA collisions is $N_{\rm part}^{pA} = N_{\rm coll}^{pA} + 1$. This relation is equivalent to Eq. (5) with $\beta = 0.5$. While this value of β in Eq. (5) underestimates data for R_h^{pA} by about one standard deviation, a larger value $\beta = 0.65$ leads to an overestimation by a similar magnitude. For further calculations we treat the interval $0.5 < \beta < 0.65$ as a measure of experimental uncertainty. This interval agrees with the multiplicity measured recently at $\sqrt{s} = 5$ TeV in [20], $dN_h^{pA}/dy = 17.24 \pm 0.66$, which leads to $\beta \approx 0.55$.

Finally we also want to relate R_h^A directly to the nuclear mass number A. We evaluate the A dependence of $N_{\rm coll}$ in Eq. (3), using as a nuclear radius $R = r_0 A^{1/3}$ with $r_0 \approx 1.12$ fm and equating the nuclear inelastic cross section with the geometrical one. Then we obtain for heavy nuclei

$$N_{\rm coll} \approx \frac{\sigma_{\rm in}^{pp}}{\pi r_0^2} A^{1/3}. \tag{6}$$

Although $N_{\rm coll}$ can be calculated much more precisely, even including Gribov corrections [21,22] and NN correlations in nuclei [23], the accuracy of calculation in (6) hardly affects the final result (see below).

III. CORRELATION BETWEEN THE MULTIPLICITY AND J/Ψ RATE ON NUCLEI

Both the J/Ψ production rate and the mean multiplicity of light hadrons in pA collisions rise with A. Here we attempt to relate them directly.

The mechanisms of the nuclear effects in J/Ψ production have been debated since the first accurate measurements at Super Proton Synchrotron in the NA3 experiment [24]. Besides the usual nuclear enhancement of hard processes by the factor $N_{\rm coll}$, the production rate of J/Ψ exposes a significant suppression, especially at forward rapidities. Depending on the collision energy, the mechanisms of suppression can include energy loss and breakup of the $\bar{c}c$ dipoles, higher twist shadowing of charm quarks and leading twist gluon shadowing (see review [25]). No consensus has been reached so far with respect to the mechanisms of J/Ψ production, either in pA or even in pp collisions. Therefore. we prefer to rely on data here.

The results of the fixed-target experiments NA3 [24] and E866 [26] on different nuclei show that the cross section of J/Ψ production on nuclei can be parametrized as A^α, so according to Eq. (2),

$$R^{pA}_{J/\Psi} \equiv \frac{\langle dN^{pA}_{J/\Psi}/dy\rangle}{\langle dN^{pp}_{J/\Psi}/dy\rangle} = \frac{N_{\rm coll}}{A}\frac{d\sigma^{pA}_{J/\Psi}/dy}{d\sigma^{pp}_{J/\Psi}/dy} = N_{\rm coll}A^{\alpha-1}, \quad (7)$$

where α depends on s and y. The results of the E866 experiment, which have the best accuracy, give $\alpha = 0.95$ at $y = 0$. NA3 data [24] at lower energy and PHENIX data [27] at $\sqrt{s} = 200$ GeV agree with this value. So far the ALICE experiment has measured J/Ψ only at forward rapidities, with a similar nuclear suppression [28].

While the first factor, $N_{\rm coll}$ in (7), is directly related to R^{pA}_h by Eq. (5), the second factor, $A^{\alpha-1}$, can be evaluated with Eq. (6). Then we arrive at

$$R^{pA}_{J/\Psi} = \left(1 + \frac{R^{pA}_h - 1}{\beta}\right)^{3\alpha-2}\left(\frac{\sigma^{pp}_{\rm in}}{\pi r_0^2}\right)^{3(1-\alpha)}. \quad (8)$$

Since the exponent in the last factor is very small, the accuracy of calculations in Eq. (6) does not affect much the result (8).

Notice that as long as α does not vary in a wide energy range, as was discussed above, the relation (8) is nearly energy independent. Indeed, the first factor apparently has no energy-dependent ingredients, only the second factor contains the slowly rising $\sigma^{pp}_{\rm in} \propto s^{0.1}$, which results in an extremely weak overall energy dependence $\propto s^{0.015}$.

The exponent α is known to vary with rapidity. It drops significantly at large Feynman x_F in the fixed-target experiments [24,26]. Moreover, data agree that α scales with x_F. However, data taken so far at RHIC and the LHC correspond to very small x_F and do not show any clear dependence of α on y. Although theoretical models predict a falling behavior of α with y, we prefer here to rely on data and provide numerical predictions only at midrapidity.

Equation (8) is the final relation between the multiplicities of J/Ψ and light hadrons in pA collisions, which we are going to apply to high-multiplicity pp collisions.

IV. BRIDGING pA AND HIGH-MULTIPLICITY pp COLLISIONS

Before one links multiparticle processes in pp and pA collisions, one may argue that there exists an essential difference. Whereas high-multiplicity pp collisions necessitate symmetric higher Fock components in both protons, pA collisions look asymmetric. Although the small-x gluon cloud from several longitudinally overlapping nucleons in a high-energy nucleus acts like a higher Fock state in a single nucleon, the proton on the other side may still be in an averaged Fock state. This argument, however, is not correct, because the weight factors for different Fock states in the proton depend on the way they are probed. The scale evolution of the parton distribution function represents a well-known example: the gluon density in the proton at small x steeply rises with the Q^2 of the photon probing it. Therefore, the mean parton configuration in the

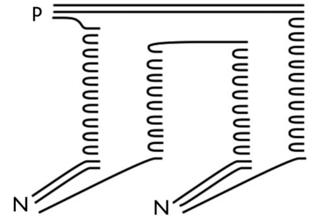

FIG. 2. Double scattering of a proton in a nucleus in the dual topological description.

proton also drifts to higher Fock components when probed by a collision with a nucleus (see Ref. [29]).

This idea is explicitly realized in the quark-gluon string [11] or dual [12] models. Multiple inelastic interactions in a pA collision are not sequential, but occur "in parallel," i.e. form a multisheet topology. Otherwise, several Pomerons could not undergo a simultaneous unitarity cut as is requested by the AGK cutting rules. An example of a double interaction of the proton with two bound nucleons [30] is depicted in Fig. 2. One can see in Fig. 2 that the proton undergoing multiple interactions has the same number of endpoints of strings as both bound nucleons together, namely two color triplets and two antitriplets. Therefore, the color content inside the proton and the nucleus for a $p - 2N$ collision looks symmetric.

Notice that semi-enhanced fan-type Reggeon graphs make the rapidity dependence of the multiplicity distribution asymmetric [31]. However, these graphs are large and the asymmetry is significant only in the nuclear fragmentation region. In the central rapidity region at high energies, the fan diagrams are suppressed by the smallness of the triple-Pomeron coupling, which originates from the smallness of gluonic dipoles within the QCD description [32].

Another source of a possible distinction between high-multiplicity pp and pA collisions is the difference in the impact parameter pattern of multiple interactions. It has been known since the early era of Regge theory that multishower particle production is characterized by smaller impact parameters of collision than in single-shower production, and this is a direct consequence of the AGK cutting rules. Indeed, the mean impact parameter squared for a single Pomeron exchange is $\langle b^2\rangle_{\bf P} = 2B_{\bf P}(s)$, where $B_{\bf P}(s) = B_0 + 2\alpha'_{\bf P}\ln(s/s_0)$ is the standard Regge parametrization for the energy-dependent elastic slope [33], $d\sigma/dt \propto \exp[B_{\bf P}(s)t]$.

The slope for the elastic amplitude with n Pomeron exchange calculated in the eikonal model is n times smaller $B_{n{\bf P}}(s) = B_{\bf P}(s)/n$. Thus, the events with multiplicity n times higher than the mean value are produced in collisions with impact parameters as small as

$$\langle b^2\rangle_{n{\bf P}} = \frac{1}{n}\langle b^2\rangle_{\bf P}. \quad (9)$$

Smallness of the mean impact parameter of a collision means larger transverse momentum of the parton,

$$\langle k_T^2 \rangle_n = n k_0^2, \quad (10)$$

where k_0 is the transverse momentum gained in a single Pomeron interaction.

On the other hand, a parton propagating through a nucleus undergoes multiple interactions with different nucleons, with impact parameters much larger than in (9). Nevertheless, the total transverse momentum gained by the parton is the same as in (10), since the single-Pomeron interaction with every nucleon remains the same, k_0. Moreover, in high-multiplicity events in pA collisions, where one should convolute multiple-Pomeron interactions with separate nucleons with increasing number of collisions, the result (10) remains valid. Indeed, comparison of $\langle k_T \rangle$ measured in pp and pA collisions at equal hadron multiplicities demonstrates the equality of the mean transverse momenta at not too large multiplicities $R_h^{pA} \lesssim 5$, which is the range of our further calculations.

However, at higher multiplicities, $\langle k_T \rangle$ in pp collisions was found to be considerably higher than in pA [34]. This remarkable observation clearly shows an onset of a new dynamics at very high R_h^{pA}, related to the existence of two scales in the proton. The semihard scale corresponds to the short-range glue-glue correlation radius [35], or the small size of instantons [36]. Small gluonic spots in the proton [32,37], which is a minor effect in the elastic pp scattering [38,39], give a significant and rising contribution at high multiplicities. They are characterized by a much higher transverse momenta of gluons and lead to a steep growth of $\langle k_T^2 \rangle$ at high multiplicities. This is a much smaller effect in pA collisions, which gain high multiplicities mainly by increasing $N_{\rm coll}$.

While these two scales affect light hadron production, they have practically no influence on the production of J/Ψ, which is characterized by an order of magnitude higher scale. For this reason, we can safely apply the results of J/Ψ production in pA collisions to high-multiplicity events in pp collisions.

V. J/Ψ PRODUCTION IN HIGH-MULTIPLICITY pp COLLISIONS

Now we are in a position to rely on nuclear effects observed (or calculated) in J/Ψ production in pA collisions, attempting to predict analogous effects in high-multiplicity pp events.

A. Production rate

We assume that the relation (8), derived for nuclear targets, can be applied to J/Ψ production in pp collisions. Within the above mentioned uncertainty in the value of β, the relation Eq. (8) is plotted in Fig. 3 as the yellow strip. We can now test our hypothesis that the dependence of $R_{J/\Psi}^{pp}$ on R_h^{pp} in pp collisions is the same as the dependence of $R_{J/\Psi}^{pA}$ on R_h^{pA} in pA collisions by comparing with data for

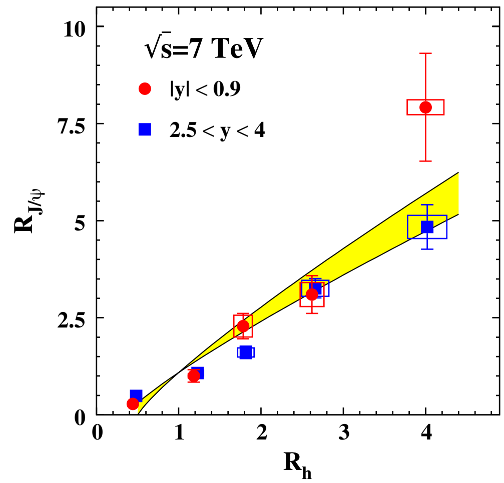

FIG. 3 (color online). Normalized multiplicity of J/Ψ, $R_{J/\Psi}$ vs normalized multiplicity of charged hadrons, R_h. Data from ALICE [40] for pp collisions at $\sqrt{s} = 7$ TeV are plotted as round points (red) for $y < 0.9$ and as squares (blue) for $2.5 < y < 4$. The upper and bottom curves show the relation (8), predicted based on data for pA collisions at $y = 0$, with $\beta = 0.5$ and 0.65 [see Eq. (5)], respectively.

high-multiplicity pp collisions [40]. We see that the dependence predicted from data on pA collisions agrees well with pp data at midrapidity. Notice that although the second factor in (8) was calculated approximately in the black disc limit, the result is rather accurate due to smallness of $1 - \alpha$.

B. p_T broadening of J/Ψ

The analogy between high-multiplicity pp events and pA collisions can be extended further. It was observed experimentally [26], and well understood theoretically [41,42], that the mean transverse momentum squared of the J/Ψ increases in pA compared to pp collisions.

As far as the gluon radiation time exceeds the nuclear size, the radiation process does not resolve between a single and multiple interactions, but is sensitive only to the total kick to the scattering color charge. For instance, if a parton gets the same momentum transfer interacting with a proton or with a nuclear target, the radiation of gluons with large $l_c \gg R_A$ should be the same. This means that multiple interactions, either in high-multiplicity pp interactions or in pA collisions, affect the p_T distribution of produced J/Ψ similarly, leading in both cases to broadening defined as

$$\Delta p_T^2 \equiv \langle p_T^2 \rangle_{R_h^{pp}>1} - \langle p_T^2 \rangle_{R_h^{pp}=1}. \quad (11)$$

The rise of the mean transverse momentum squared, for a gluon propagating through a nucleus at impact parameter b, was calculated in [41–43] as

$$\Delta p_T^2(b) = \frac{9}{2} C(E) T_A(b), \quad (12)$$

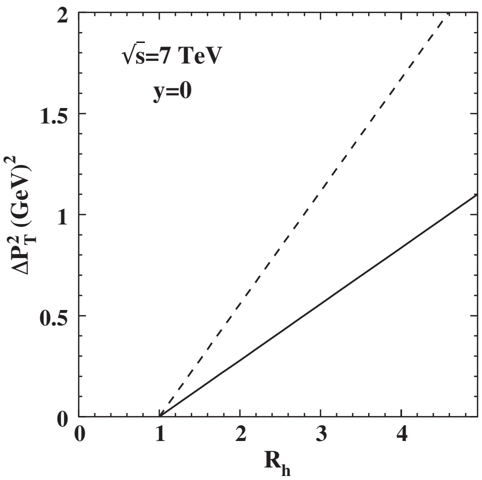

FIG. 4. p_T broadening of J/Ψ produced in high-multiplicity pp collisions at $\sqrt{s} = 7$ TeV at midrapidity. The solid and dashed curves present broadening calculated with Eq. (14), including or excluding the corrections for gluon shadowing.

where E is the gluon energy in the nuclear rest frame and the nuclear thickness function $T_A(b) = \int_{-\infty}^{\infty} dz \rho_A(b, z)$ is given by the integral of the nuclear density ρ_A along the parton trajectory.

The coefficient $C(s)$ controls the behavior of the universal dipole cross section at small dipole sizes,

$$C(E) = \frac{1}{2} \vec{\nabla}_{r_1} \cdot \vec{\nabla}_{r_2} \sigma_{\bar{q}q}(\vec{r}_1 - \vec{r}_2, E) \Big|_{\vec{r}_1 = \vec{r}_2}. \quad (13)$$

This factor steeply rises with energy. For J/Ψ produced at $\sqrt{s} = 7$ TeV at the midrapidity, $E = e^y \sqrt{s(M_{J/\Psi}^2 + \langle p_T^2 \rangle)}/2m_N = 15.6\ \mathrm{TeV} \times e^y$. At this energy and $y = 0$, the factor $C(E)$ was calculated in [42] at $C(E) = 13$. Inclusion of gluon shadowing corrections [42] substantially reduces this factor $C(E) \Rightarrow C_{\mathrm{shad}} = 6.5$. We rely on this value for further evaluations.

Broadening Eq. (12) averaged over impact parameter is given by the mean number of collisions, Eq. (3),

$$\Delta p_T^2 = \frac{9 C_{\mathrm{shad}}}{2 \sigma_{\mathrm{in}}^{pp}} (N_{\mathrm{coll}} - 1) = \frac{9 C_{\mathrm{shad}}}{2 \sigma_{\mathrm{in}}^{pp} \beta} (R_h^{pA} - 1). \quad (14)$$

The expected broadening of J/Ψ produced in high-multiplicity pp collisions at $\sqrt{s} = 7$ TeV and $y = 0$ is plotted in Fig. 4 as a solid line, as a function of the normalized multiplicity R_h^{pp}. Calculations are done with $\beta = 0.6$. The dashed line shows, for comparison, broadening calculated without shadowing corrections.

VI. SUMMARY

High-multiplicity pp collisions at high energies exhibit features that traditionally have been associated with nuclear effects. Here we observed a close similarity between multiple interactions in pp and pA collisions. In order to enhance multiple interactions in the former case, one should trigger on high multiplicity of produced hadrons, while in the latter case one can reach the same multiplicity due to the increased number of collisions [Eq. (3)]. We employed the phenomenological description of the mean multiplicity in pA collisions, Eq. (5), and the observed nuclear effects for J/Ψ production, enabling us to predict the multiplicity dependence of the J/Ψ production rate in pp collisions. The results agree well with the correlation between $R_{J/\Psi}^{pp}$ and R_h^{pp} observed in pp collisions at the LHC [40].

Notice that the observed behavior of the relative J/Ψ yield vs hadron multiplicity is not trivial and is under debate in the literature. In particular, the PYTHIA event generator predicts an opposite behavior, a falling multiplicity dependence of the relative production rate of J/Ψ (see Fig. 4 in [40]). Although an alternative interpretation, the effect of multiparton interactions, was discussed in [40], this mechanism has not been considered for J/Ψ production in pA collisions so far, and no numerical prediction for high-multiplicity pp events has been provided.

We also predicted p_T broadening for J/Ψ produced in high-multiplicity, compared with mean-multiplicity, pp collisions. We relied on data at midrapidity, since the possible rapidity dependence of α at the LHC energy is poorly known. If, however, the value of α drops at forward rapidities, this will lead to smaller values of $R_{J/\Psi}^{pA}$ at large multiplicities. Although we employed data for pA collisions integrated over the impact parameter, the analysis can be done at different centralities.

ACKNOWLEDGMENTS

This work was supported in part by Fondecyt (Chile) Grants No. 1130543, No. 1130549, No. 1100287 and by Conicyt-DFG Grant No. RE 3513/1-1.

[1] O. V. Kancheli, Pis'ma Zh. Eksp. Teor. Fiz. **18**, 465 (1973) [JETP Lett. **18**, 274 (1973)].
[2] V. A. Abramovskii and O. V. Kancheli, Pis'ma Zh. Eksp. Teor. Fiz. **15**, 559 (1972).
[3] K. A. Ter-Martirosyan, Phys. Lett. **44B**, 377 (1973).
[4] A. B. Kaidalov and K. A. Ter-Martirosian, Phys. Lett. **117B**, 247 (1982).
[5] V. A. Abramovsky, V. N. Gribov, and O. V. Kancheli, Yad. Fiz. **18**, 595 (1973) [Sov. J. Nucl. Phys. **18**, 308 (1974)].

[6] K. A. Ter-Martirosyan, Pis'ma Zh. Eksp. Teor. Fiz. **15**, 734 (1972).

[7] O. V. Kancheli, Pis'ma Zh. Eksp. Teor. Fiz. **11**, 397 (1970) [JETP Lett. **11**, 267 (1970).

[8] A. H. Mueller, Phys. Rev. D **2**, 2963 (1970).

[9] W. Q. Chao, M. K. Hegab, and J. Hüfner, Nucl. Phys. **A395**, 482 (1983).

[10] M. S. Dubovikov, B. Z. Kopeliovich, L. I. Lapidus, and K. A. Ter-Martirosian, Nucl. Phys. **B123**, 147 (1977).

[11] A. B. Kaidalov, JETP Lett. **32**, 474 (1980) [Sov. J. Nucl. Phys. **33**, 733 (1981); Phys. Lett. **116B**, 459 (1982).

[12] A. Capella, U. Sukhatme, C.-I. Tan, and J. Tran Thanh Van, Phys. Rep. **236**, 225 (1994).

[13] A. B. Kaidalov, Phys. Lett. **116B**, 459 (1982).

[14] A. B. Kaidalov and K. A. Ter-Martirosian, Yad. Fiz. **39**, 1545 (1984) [Sov. J. Nucl. Phys. **39**, 979 (1984)].Yad. Fiz. **40**, 211 (1984) [Sov. J. Nucl. Phys. **40**, 135 (1984).

[15] L. V. Gribov, E. M. Levin, and M. G. Ryskin, Nucl. Phys. **B188**, 555 (1981); Phys. Rep. **100**, 1 (1983).

[16] A. H. Mueller, arXiv:hep-ph/9911289.

[17] L. D. McLerran and R. Venugopalan, Phys. Rev. D **49**, 2233 (1994); Phys. Rev. D **49**, 3352 (1994); **50**, 2225 (1994).

[18] J. E. Elias, W. Busza, C. Halliwell, D. Luckey, P. Swartz, L. Votta, and C. Young, Phys. Rev. D **22**, 13 (1980).

[19] B. B. Back *et al.* (PHOBOS Collaboration), Phys. Rev. C **72**, 031901 (2005).

[20] B. Abelev *et al.* (ALICE Collaboration), Phys. Rev. Lett. **110**, 032301 (2013).

[21] B. Z. Kopeliovich, Phys. Rev. C **68**, 044906 (2003).

[22] B. Z. Kopeliovich, I. K. Potashnikova, and I. Schmidt, Phys. Rev. C **73**, 034901 (2006).

[23] C. Ciofi degli Atti, B. Z. Kopeliovich, C. B. Mezzetti, I. K. Potashnikova, and I. Schmidt, Phys. Rev. C **84**, 025205 (2011).

[24] J. Badier *et al.* (NA3 Collaboration), Z. Phys. C **20**, 101 (1983).

[25] B. Z. Kopeliovich, Nucl. Phys. **A854**, 187 (2011).

[26] M. J. Leitch *et al.* (FNAL E866 Collaboration), Phys. Rev. Lett. **84**, 3256 (2000).

[27] A. Adare *et al.* (PHENIX Collaboration), Phys. Rev. Lett. **107**, 142301 (2011).

[28] B. B. Abelev *et al.* (ALICE Collaboration), arXiv:1308.6726.

[29] B. Z. Kopeliovich, H. J. Pirner, I. K. Potashnikova, and I. Schmidt, Phys. Lett. B **697**, 333 (2011).

[30] A. Capella and B. Z. Kopeliovich, Phys. Lett. B **381**, 325 (1996).

[31] J. Koplik and A. H. Mueller, Phys. Rev. D **12**, 3638 (1975).

[32] B. Z. Kopeliovich, I. K. Potashnikova, B. Povh, and I. Schmidt, Phys. Rev. D **76**, 094020 (2007).

[33] K. G. Boreskov, A. B. Kaidalov, and O. V. Kancheli, Yad. Fiz. **69**, 1802 (2006) Phys. At. Nucl. **69**, 1765 (2006).

[34] B. Abelev *et al.* (ALICE Collaboration), arXiv:1307.1094.

[35] A. DiGiacomo and H. Panagopoulos, Phys. Lett. B **285**, 133 (1992).

[36] E. Shuryak and I. Zahed, Phys. Rev. D **69**, 014011 (2004).

[37] B. Z. Kopeliovich, A. Schäfer, and A. V. Tarasov, Phys. Rev. D **62**, 054022 (2000).

[38] B. Z. Kopeliovich, I. K. Potashnikova, B. Povh, and E. Predazzi, Phys. Rev. Lett. **85**, 507 (2000); Phys. Rev. D **63**, 054001 (2001).

[39] B. Z. Kopeliovich, I. K. Potashnikova, and B. Povh, Phys. Rev. D **86**, 051502 (2012).

[40] B. Abelev *et al.* (ALICE Collaboration), Phys. Lett. B **712**, 165 (2012).

[41] M. B. Johnson, B. Z. Kopeliovich, and A. V. Tarasov, Phys. Rev. C **63**, 035203 (2001).

[42] B. Z. Kopeliovich, I. K. Potashnikova, and I. Schmidt, Phys. Rev. C **81**, 035204 (2010).

[43] J. Dolejsi, J. Hüfner, and B. Z. Kopeliovich, Phys. Lett. B **312**, 235 (1993).